Comparative analysis for bus side structures and lightweight optimization

F Lan[1]*, **J Chen**[1] and **J Lin**[2]
[1]The School of Automotive Engineering, Jilin University, Changchun, People's Republic of China
[2]Mechanical and Manufacturing Engineering, University of Birmingham, Birmingham, UK

Abstract: Lightweight structures in bus body design have been highlighted. In this investigation a new typical medium-sized bus body structure has been modelled and analysed using the computer aided design (CAD) package UG and finite element (FE) solver ANSYS. This paper presents a comparative analysis of two body side structures: with and without structural supporting members between the longitudinal waist beams of the side frames. Firstly, analysis of structure strength and stiffness for low-order vibration modes was carried out, and the effects of different structures on strength, rigidity and material use efficiency were examined. Corresponding experimentation was carried out to validate the simulation results. Secondly, sensitivity studies and structural optimization were performed to reduce body weight without losing overall strength and rigidity. Geometric parameters, including cross-sectional parameters and wall thickness, of large structural members are considered in the optimization. The results of the research provide a means of structural design optimization with consideration of bus body weight reduction.

Keywords: body structure, stress, stiffness, finite element, structural optimization, lightweight

1 INTRODUCTION

Recently, significant efforts have been made by automotive manufacturers to meet the increasing need to reduce production costs and improve fuel efficiency [1, 2]. Weight reduction of vehicle body structures is pursued as one of the solutions to meet the requirements, and the lightweight design of autobody structures has become an important issue for this purpose [2–6]. In order to achieve a significant reduction in vehicle weight, two aspects need to be considered:

(a) the application of alternative lighter materials such as aluminium and composites replacing conventional steels [2];
(b) a reduction in the number and weight of parts in the whole body structure without replacing steel [3–6].

The investigation in this paper is concerned with the latter, which not only reduces the production cost reasonably but also avoids extra tooling investments due to the replacement of material and the corresponding changes

in joining technology. However, simple modification of structural parts may be limited by the body strength, stiffness and crashworthiness. Therefore, an understanding of the detailed strength and stiffness distribution in a body is important for attaining optimization in weight reduction design and effective structural strength and rigidity. The finite element (FE) method has usually been employed as a means to this end and is validated by experimental studies [4–12].

The body structure chosen in the present investigation is a medium-sized bus newly developed by one of the biggest passenger car manufacturers in China. It adopts a non-load-supporting structural frame on a specialized bus chassis, described as having good seating comfort and aesthetic appearance. In order to ensure both the required reliability of body performance and efficient use of material, a synthetic comparative study on body rigidity and strength, load-carrying capacity and design optimization has been carried out with combined theoretical and experimental approaches. This is done by analysing the difference in load-carrying capacity (rigidity and strength) between an actual bus body and a modified design structure (that has a number of skewed supporting rods connecting the long longitudinal beams at the waist part of the sides removed). The vibration modes between the alternative structures are analysed. Optimization and sensitivity analysis are carried out

on body structural parameters with the objective of minimizing body weight while retaining the required performance. Finally, some targets and measures are proposed that may provide designers with relevant structural parameters to improve design reliability and reduce design lead time for a new product.

2 FE ANALYSIS

Detailed modelling is processed as follows:

(a) the generation of a detailed body geometric model using the computer aided design (CAD) system UG (Fig. 1);
(b) the creation of a mesh using the preprocessor PATRAN, which is then implemented into the FE solver ANSYS for FE analysis.

The FE model for the body structure is shown in Fig. 2. It contains 44 930 elastic four-noded shell elements (SHELL63), 44 elastic three-noded beam elements (BEAM4) and four spring elements (COMIN14). In the FE model, each member of the body structure uses actual thickness values and material property parameters, for example: material Q235, Young's modulus 2.06×10^{11} Pa, density 7.85×10^3 kg/m^3, Poisson's ratio 0.3 and static yield stress 295 MPa.

There are two main loading cases: the bending case, which is the most frequent case in normal use of vehicles, and the torsional case, which generally results in large stress in a bus body. The present investigation selects the fully loaded bending case (abbreviated as the 'bending cas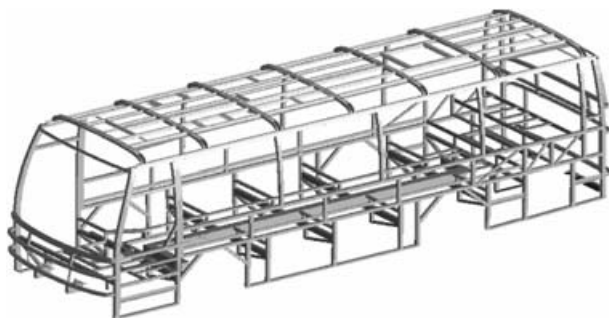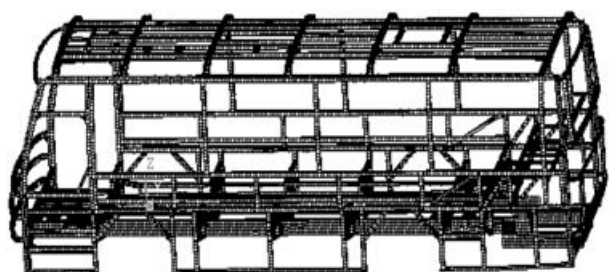e') and the fully loaded torsional case with the front left wheel off the ground (abbreviated as the 'torsional case'), which are extreme loading cases in actual operation. Body self-weight, assembly parts and passenger weight act as the major bending load. The loads of the body structural parts are simulated by using a vertical acceleration of 9.8 m/s^2, and the equivalent contacts between passengers and seats are applied on the corresponding nodes in terms of their individual positions and weights, where the passenger mass is $34 \times 65 = 2210$ kg, the seat mass is 680 kg and the other assembly masses are as follows: engine 580 kg, gearbox 100 kg, fuel tank 150 kg, steering system 100 kg, radiator 50 kg, single wheel 60 kg, clutch 70 kg, compressor 100 kg, battery 70 kg, air conditioning 200 kg and heating system 700 kg. The whole bus is simulated as a free beam system throughout the analysis process, where the stiffnesses of the plate springs and tyres are also needed the plate spring stiffness is 163 N/mm (front) and 326.67 N/mm (rear) and the tyre stiffness is 635 N/mm.

The body skeleton density K is an important factor for assessing material use efficiency, which is defined as $K = W/L$, where W is the body structure mass (kg) and L is the body length (m). If it is small enough, the load-carrying capability can be fully employed, otherwise the material use efficiency might be low. In general, the body skeleton density, K, lies in the range 110–170 kg/m, and the average is around 139 kg/m. The density of this actual bus model is 153.8 kg/m, which is higher than average. This suggests that the material capacity has not been fully used, and further design optimization is required to enable a lightweight body structure to be achieved.

2.1 Bending case

2.1.1 Bending rigidity

The bending rigidity of an autobody is very important for body performance. In the fully loaded bending case, the vertical deflections of the left and right longitudinal beams are shown in Fig. 3, where the X axis value, 'point numbering', is the order of the calculated points from the front to the rear along the long longitudinal beams.
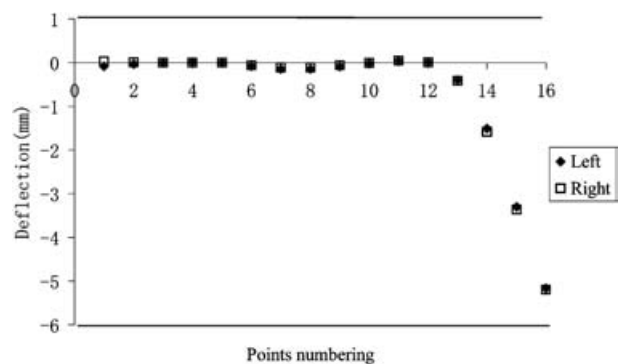

Fig. 1   CAD model of the body structure

Fig. 2   FE model of the body structure

Fig. 3   Deflections of the left and right longitudinal beams in the bending case
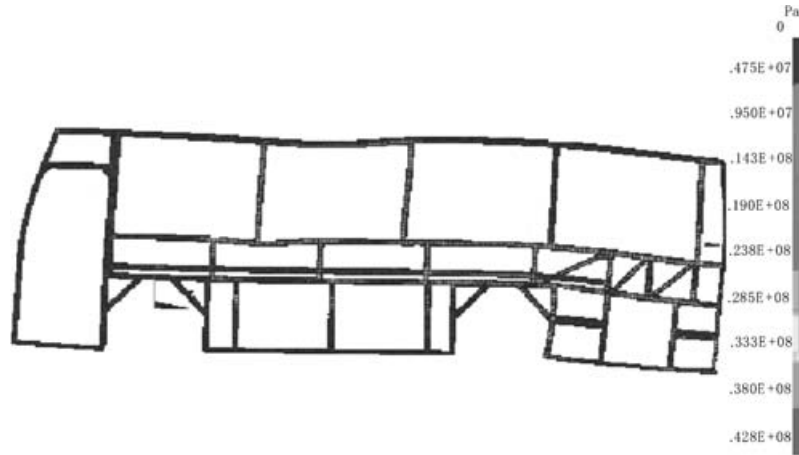
Fig. 4 Stress distribution over the (right) side for the bending case

The following results are obtained from the analysis:

1. A uniform variation in the deflections shows that the bending rigidity of the body is also evenly distributed along the longitudinal direction.
2. A change in direction of the curves occurs near the centres of the front and rear axle shafts (points 4 and 11), and the deflection values increase between points 11 to 16. This reflects the actual loading situation resulting from the concentrated loads of engine, gearbox and radiator, all acting on the rear part of the chassis.
3. The deflection of the right longitudinal beam is slightly larger than that of the left because of the door opening on the right, which results in a slightly lower bending rigidity on that side.

2.1.2 Bending stress

In the case of bending, the stress level is usually lower than 10 MPa on the sides, the roof and the front and rear panels, and the stress distribution on the side panel is shown in Fig. 4. In most of the chassis frame the stress level is lower than 10 MPa, although it is slightly higher in some local regions. The high stress regions on the side panels above the chassis frame occur at:

1. The sections of connections between the vertical posts of the side window frames and two longitudinal beams. The average stress is around 20 MPa.
2. The sections of connections between the vertical middle posts, the lower beam of the window frames and the middle longitudinal beam. The average stress is around 30 MPa.

The highest left side stress is about 61 MPa and occurs at the point of connection between the second vertical middle post and the middle longitudinal beam. The highest right side stress is around 44 MPa and occurs at the point of connection between the third vertical middle

post and the middle longitudinal beam. Other relevant high stress values and locations will be shown in the later trade-off study with experimental results.

2.2 Torsional case

2.2.1 Torsional rigidity

Torsional rigidity is also important for bus body performance. Figure 5 shows the changes in the bus body torsional angle:

1. A uniform variation in the body torsional angles shows that the torsional rigidity of the body is evenly distributed along the longitudinal direction.
2. Some changes still occur at points 4 and 11 owing to the constraints at the centres of the front and rear axle shafts.
3. The torsional angle increases from point 11 to point 16 as a result of the concentrated loads of the engine, gearbox, radiator, etc.

Through the comparison of the body torsional angle between the two body structures (with and without supporting members on the side frames), the following results can be obtained (Fig. 5):
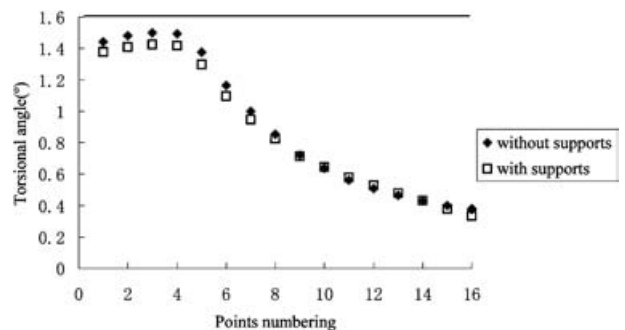

Fig. 5 Body torsional angles between the axle shafts with and without supporting members
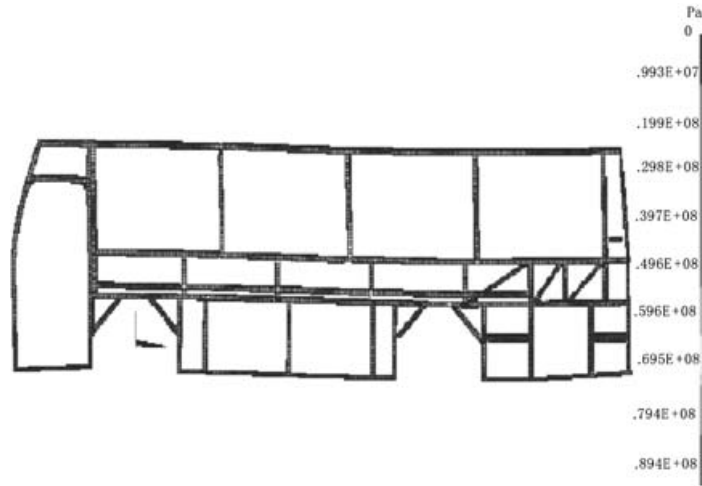
Fig. 6 Stress distribution over the left side for the torsional case

1. The torsional rigidity does not change significantly after removal of some of the supporting members between the middle longitudinal beams.
2. The body torsional angles change more evenly after removal of some of the supporting members, i.e. the body torsional rigidity is still uniformly distributed, just slightly lower.

The body torsional rigidity, after removal of some of the supports, is 2.1205×10^4 N m/deg. As known in the general legislation for a semi-load-supporting passenger automotive body, the torsional rigidity between the axle shafts is better in the range $1.8–4.0 \times 10^4$ N m/deg, so the bus body meets this requirement.

2.2.2 Torsional stress

The torsional case has a similar stress distribution over the bus body above the chassis frame to the bending case, but the amplitude tends to be higher. The reason is that the torsional case is one of the worst cases, and hardly ever happens with a single wheel off the ground during actual running.

The highest left side stress, 61 MPa, is at the connection between the second vertical middle post and the middle longitudinal beam; the highest right side stress, 78 MPa, is at the section of connection between the third vertical middle post and the middle longitudinal beam (Fig. 6). Other relevant high stress values and locations will be shown in the later trade-off study with experimental results.

2.3 Strength comparison

Considering that the bending cases have the same stress trend as the torsional cases in the high-stress sections, the torsional case is selected for this strength trade-off analysis to simplify the calculation process. Figures 7
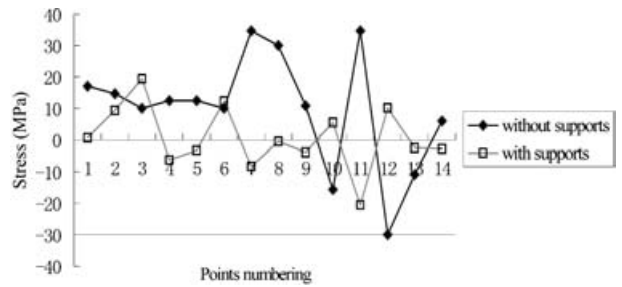

Fig. 7 Left side stress in the two structures

and 8 show the stress results of the measured points on the two structural models (with and without supporting members).

According to the distribution of the measured points, some points are taken for their stress comparison: on the left side, points 4, 5, 6, 9, 10, 11, 12, 15, 16, 17, 18, 19 and 20; on the right side, points 6, 7, 8, 9, 12, 13, 14, 15, 18, 19, 20, 21, 22 and 23. This comparison indicates that, with the supports, the structure stress is lower at most of the measured points, but after removal of the supports the stress is still low enough compared with the yield stress, so the strength remains satisfactory.
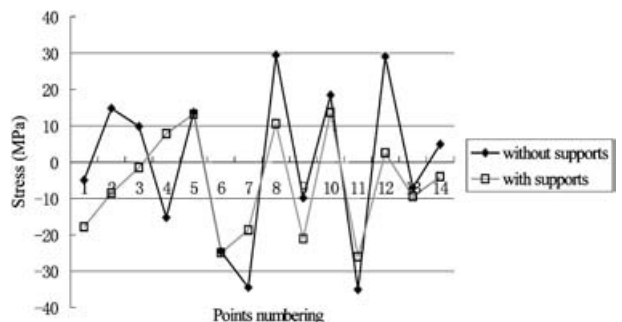

Fig. 8 Right side stress in the two structures

2.4 Modal analysis of low-order vibration modes

In the modal analysis, a simplified FE model (Fig. 9) is used. Through observing and understanding the lower-order vibration modes, Table 1 lists the details of the frequencies of the lowest six modes for the two structural models (Fig. 10 shows the fundamental mode). Comparing the results for the two structures, it can be seen that there is no sharp local change in these modes, i.e. the rigidity distribution is uniform over the whole body with the fore/aft supports removed.

2.5 Result summary

The rigidity distribution over the whole body remains uniform with no major changes, and the body rigidity is higher relative to the chassis frame. The stress level over the whole body is still low enough after removal of the supports, but is marginally less evenly distributed. However, the stress at the connections between the window frames, the vertical middle posts and the middle longitudinal beams remains high. Overall, the main causes for the high stress sections in the bending and torsional cases might be due to the typically weak side window regions. The bus body has large side windows and uses direct welding joining of rectangular tubes without smooth fillets, so high stress sections are caused
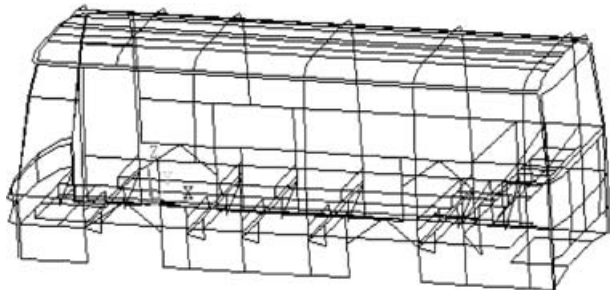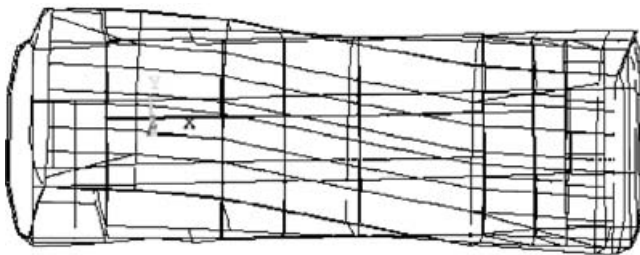
as a result of structural deformation. As the engine is rear positioned, the long rear suspension frame (2400 mm) carries the largest concentrated loads. Thus, the deformation in the rear part is like that of a cantilever, and the post-bridge supporting point is where the high stress occurs.

The analysis results illustrate that the rigidity and strength of the bus body structure satisfy the design requirements, and the stress and deformation within the structure are relatively low. This indicates that the load-carrying capability of the material has not been fully utilized.

3 EXPERIMENTAL STUDY

Static and dynamic tests are carried out on the bus, shown in Fig. 11, to validate the analysis results for the structural modifications. The body static experiment is to measure the structural stress distribution under various static loading cases. High stress concentration regions in the body are key points to be measured, such as the corners of doors, welding sections of the vertical posts of windows, etc. Based on experience and the previous FE results, 64 points are selected for the experimental measurement, which are detailed in Figs 12 and 13.

To enable direct comparison between computational and experimental results to be carried out, stress values calculated using ANSYS are produced for the points of experimentally measured elements of the body structure. For the bending tests, the loads are simulated to the real situation: a weight-equivalent sand bag, 65 kg on each seat. The same loading case is used for the torsional tests, where the left front wheel is lifted off the ground.

Fig. 9   Simplified FE model of the body

Fig. 10   Fundamental mode of the body

Fig. 11   Sample bus for testing

Table 1   Frequencies of the lowest six modes (Hz)

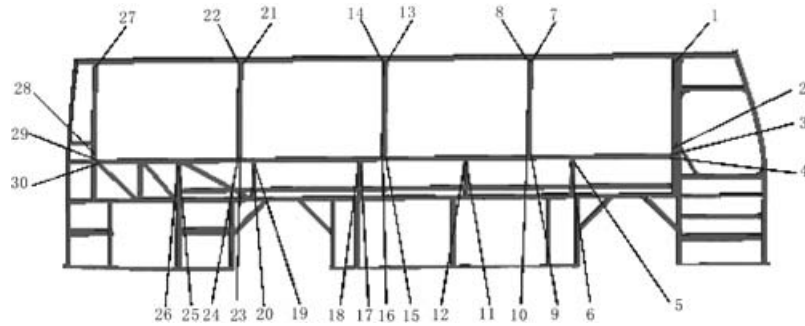|	Mode					
	First	Second	Third	Fourth	Fifth	Sixth
Without supports	12.867	18.92	20.151	21.466	21.642	23.638
With supports	13.098	19.143	21.441	21.922	23.574	24.594

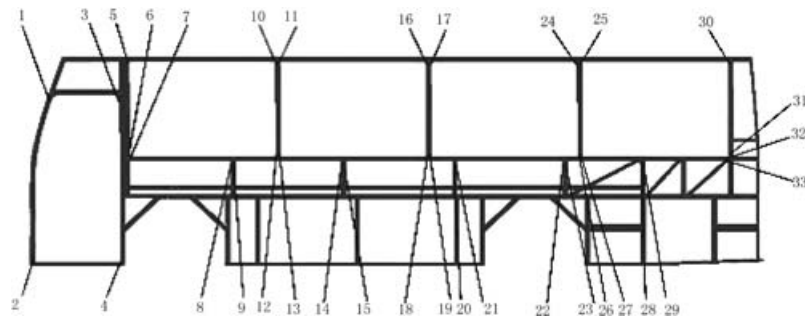**Fig. 12**   Experimental measurement points at the left side

Fig. 13   Experimental measurement points at the right side

3.1   Static test

In the strength tests, strains are measured at the specified locations shown in Figs 12 and 13. At each defined point, strains are measured in three different directions using strain rosettes. In a two-dimensional system of stresses there are always two perpendicular directions, where shear stresses are zero and principal stresses σ_1 and σ_2 can be defined. The von Mises stresses, which are compared with FE results, are then calculated according to the principal stresses.

Comparisons of experimental and computational stresses for the corresponding points are shown in Figs 14 and 15. In the bending case (Fig. 14), the highest stress of the left side is at the location of the connection between the third and fourth vertical posts and the window frame beams. The highest stress level is about 90 MPa. On the right side the highest stress, which is
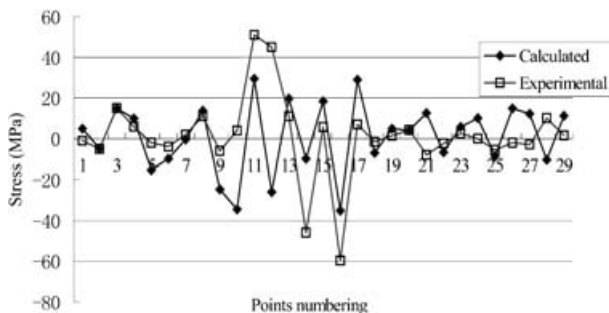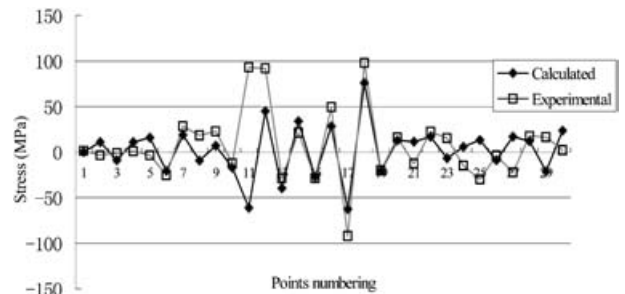

Fig. 15   Stress comparison on the right side for the torsional case

around 60 MPa, occurs at the same locations. Generally speaking, the structure over the chassis frame of the bus body has low stresses, but the stress distribution is not ideally uniform. In the torsional case the experimental data (Fig. 15) also show that the highest left side stress is about 105 MPa, which occurs at the sections of connection between the third vertical middle post and the window frame beams. On the right side the highest stress is about 98 MPa, which occurs at similar locations on the other side. Moreover, the stress in the rear suspension regions of both sides is usually high, especially at the sections of connection between the supports and the vertical middle posts and the middle longitudinal beam, where the average stress is around 60 MPa on the left side and 20 MPa on the right. The results show a correlation with their trends, except a few anomalous points, where further experiments and calculations are required.

Fig. 14   Stress comparison on the left side for the bending case

3.2 Dynamic experiment

Dynamic experiments to investigate structural modifications are undertaken under the two typical conditions—bad and good roads. Figures 16 to 18 present the peak values which show the stress of the measured points (driving speeds 50 and 85 km/h).
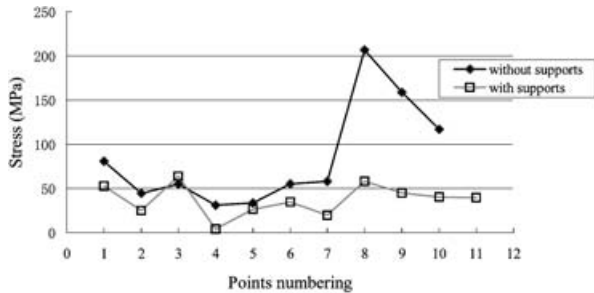

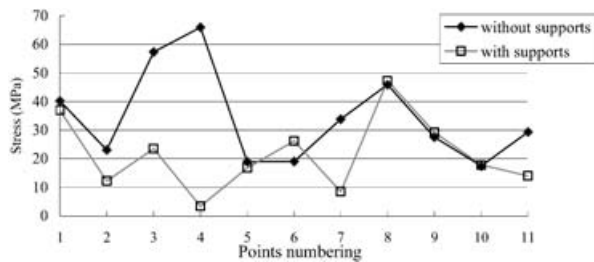**Fig. 16** Stress of the measured points on a bad road

Fig. 17 Stress of the measured points on a good road (driving speed 50 km/h)
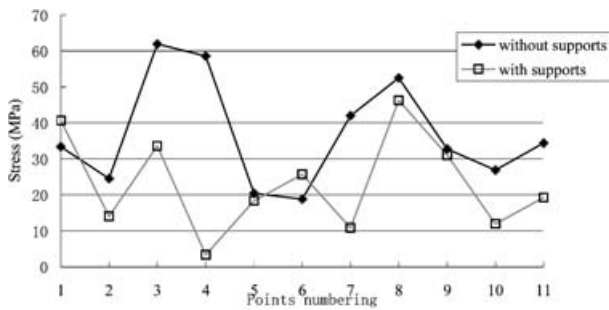

Fig. 18 Stress of the measured points on a good road (driving speed 85 km/h)

The dynamic stress result shows that the stresses at most of the measured points are lower in the bus body with the supports than without the supports, i.e. the supports could act as some reinforcement of the body. However, the highest stress is still lower than the material yield stress (295 MPa), which meets the design specification.

4 BODY LIGHTWEIGHT OPTIMIZATION

Although the rigidity and the strength of the body have satisfied the design specifications, both the body skeleton weight and the density are too high, i.e. the material capability has not been efficiently utilized. Currently, a promising design is pursuing this objective to generate a lighter-weight and lower-cost body. Thus, it is expected that, apart from satisfying the performance required in operation, optimization analysis is able to reduce the weight of structural components and increase the load-carrying efficiency of the material.

4.1 Sensitivity analysis

This optimization is carried out with a simplified structural model where beam elements make up the main application. In accordance with previous results, box-type beams of large cross-section are selected for optimization. This involves a total of eight groups, and the wall thickness of the beams is an objective parameter to be optimized. The sensitivity of wall thickness to body performance is studied. The selected components are: the upper cross-beam of the chassis frame (TK1), the lower frames of the side windows (TK2), the middle longitudinal beams (TK3), the vertical middle posts (TK4), the lower frame of the back window (TK5), the upper and lower frames of the radiator supporting structure (TK6), the bridging bars of the chassis frame (TK7) and the lower cross-beam of the chassis frame (TK8). Detailed analysis of the parameters shows the sensitivity to the rigidity and the mass of the structure, which are given in Table 2 (TK represents thickness).

The cross-sectional features affect the body torsional rigidity, the fundamental torsional frequency and the total mass of the body. It is expected that, as the body

Table 2 Sensitivity of cross-sectional parameters to rigidity and weight

Component	Design variables		Torsional rigidity		Weight		Rigidity/ weight
	Initial (m)	Variation (m)	Variation (N m/deg)	Sensitivity	Variation (kg)	Sensitivity	
TK1	0.004	0.5E-5	4.4712	8.94E5	0.08775	1.76E4	51
TK2	0.0015	0.25E-5	0.558	2.23E5	0.04986	1.99E4	11.2
TK3	0.0015	0.25E-5	0.8596	3.44E5	0.06177	2.47E4	13.9
TK4	0.0015	0.25E-5	2.3784	9.51E5	0.03307	1.32E4	71.9
TK5	0.0015	0.25E-5	0.0252	1.01E4	0.01759	7.04E4	1.43
TK6	0.0015	0.25E-5	0.2759	1.1E5	0.02854	1.14E4	9.67
TK7	0.0015	0.25E-5	4.8128	1.93E6	0.03619	1.45E4	133
TK8	0.0015	0.25E-5	6.8377	2.74E6	0.08217	3.29E4	83.2

rigidity and the fundamental frequency are improved, the mass will remain constant or decrease. Thus, to assess the sensitivity of the changes, two ratios, rigidity/weight and frequency/weight, are introduced and known as sensitivity ratios. The rigidity/weight ratio is defined as 'sensitivity gradient to rigidity/sensitivity gradient to weight', and the frequency/weight ratio is defined as 'sensitivity gradient to frequency/sensitivity gradient to weight'. In this paper the two ratios are also referred to as 'sensitivity ratios'.

The sensitivity of the cross-sections is related to the body torsional rigidity (Fig. 19) and to the rigidity/weight ratio (Fig. 20). The cross-sectional parameters TK1, TK4, TK7 and TK8 are more sensitive than the others to both rigidity and the rigidity/weight ratio. Thus, owing to the different sensitivities, an optimization process can be carried out by means of different specially selected parameters of the components.
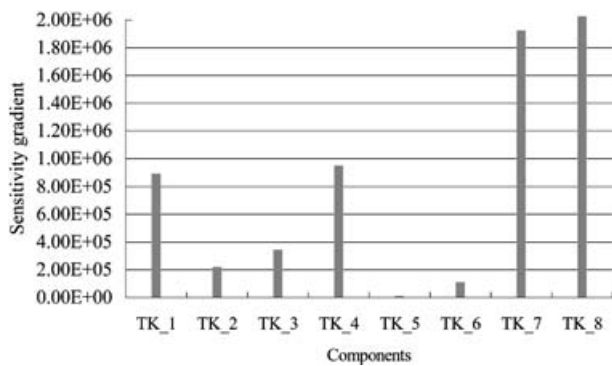

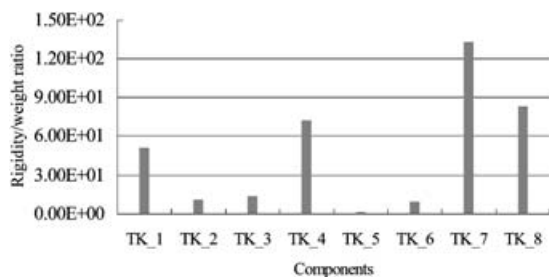Fig. 19   Sensitivity of the torsional rigidity

Fig. 20   Sensitivity of rigidity/weight

Figure 21 shows the sensitivity of the cross-sectional parameters to the frequency/weight ratio. The parameters sensitive to rigidity/weight are also sensitive to frequency/weight. However, different parameters have differing effects on the sensitivity results. During the optimization process it is necessary to consider the influence of the cross-sectional features on different sensitivities. It is better to select those parameters that are more sensitive to the various sensitivity variables. As shown by the results, TK1, TK4, TK7 and TK8 are more sensitive to the various sensitivity variables, but TK5 is sensitive only to frequency and weight. This provides a valuable reference for the following optimization.

4.2   Body weight optimization

The objective of the optimization is to lighten the body skeleton mass. As the material density of 7850 kg/m^3 is already known, the skeleton weight (WT) will be the objective function. The whole body torsional rigidity (TSTFF) and the fundamental torsional frequency (MODEL7) are the state functions in terms of their effects on the body structural performance. According to the above sensitivity analysis, the optimized objects are the lower frame beams of the side windows, the middle longitudinal beam, the vertical middle posts, the upper and lower cross-beams of the chassis frame and the bridging bars of the chassis frame, and their cross-sectional width (B) and wall thickness (TK). The objective function, state function, design variables and optimization results are shown in Table 3.
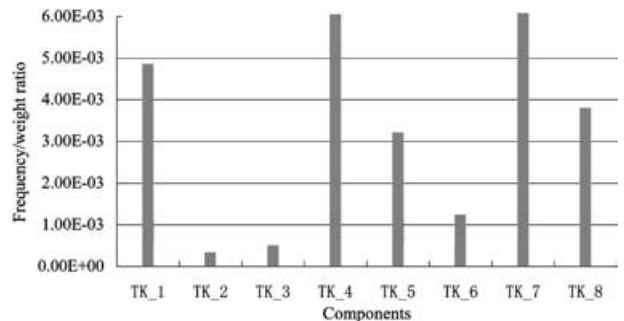

Fig. 21   Sensitivity of frequency/weight

Table 3   Body structure weight optimization process

Optimized variables	Code	Initials	Minimum limit	Maximum limit	Convergence accuracy	Results
Objective function	WT (kg)	1155.96			0.10	1089.9
State function	TSTFF (N m/deg)	22 868.8	28 000	35 000	0.10	20 267
	MODEL7 (Hz)	12.867	10	15	0.10	12.42
Design variables	B (m)	0.005	0.005	0.004	0.10E-03	0.004
	TK2/3 (m)	0.0015	0.0015	0.001	0.10E-03	0.001
	TK1 (m)	0.004	0.004	0.003	0.10E-03	0.001
	TK4 (m)	0.0015	0.0015	0.001	0.10E-03	0.001
	TK7 (m)	0.0015	0.0015	0.001	0.10E-03	0.001
	TK8 (m)	0.0015	0.0015	0.001	0.10E-03	0.001

The body torsional rigidity (2602 N m/deg), the body weight (66 kg) and the fundamental frequency (0.45 Hz) decrease by 11 per cent, by 5.7 per cent and by 3.5 per cent respectively. The weights of the eight groups of components have little effect on the lower-order frequencies but a greater effect on the torsional rigidity, which matches the results of the sensitivity analysis of torsional rigidity. Figure 22 shows the convergence process of the body weight for the six design variables.

5 CONCLUSIONS

A trade-off study between two different body structures, road tests and finally lightweight optimization design have been carried out. The following conclusions can be drawn:

1. The bus body structure is widely used, and therefore the analysis carried out in the present investigation has widespread significance for bus design and manufacture. The body strength capability reserve was in excess of the performance requirement. As there is constant improvement in actual road condition and loading arrangement, future structural improvement strategy is likely to focus on increasing the whole body performance and product competitive ability through both reducing structural weight and increasing rigidity.
2. The structural alternative without supporting members is suggested as being the most valuable application, enabling both significant alleviation of body weight and satisfactory performance requirements of the load-carrying capability.
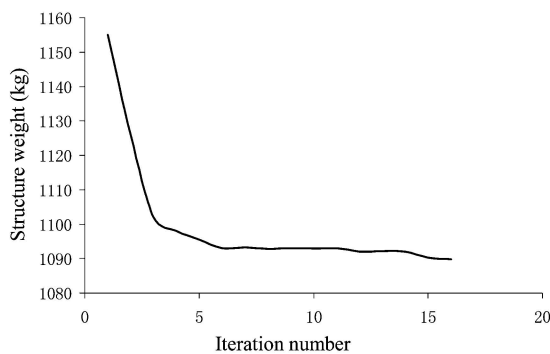

Fig. 22 Body weight convergence curve

3. The cross-sectional features of the structural members have various effects on the body performance. Therefore, attention to the selection of objective functions and boundary conditions for design parameter optimization will make the solutions more effective and rational in overcoming the possible shortcomings of traditional and experience-based designs.

REFERENCES

1 **Matthews, A. E.** Fuel efficient sheet steel automobiles. *New and Alternative Mater. for Transpn Industries*, 1994, 163–164.
2 **Saito, M., Iwatsuki, S., Yasunaga, K.** and **Andoh, K.** Development of aluminium body for the most fuel efficient vehicle. *JSAE Rev.*, 2000, **21**, 511–516.
3 **Takamatsu, M.** Development of lighter-weight, higher-stiffness body for new RX-7. SAE paper 920244, 1992.
4 **Pine, T., Lee, M. M. K.** and **Jones, T. B.** Weight reduction in automobile structures—an experimental study on torsional stiffness of box sections. *Proc. Instn Mech. Engrs, Part D: J. Automotive Engineering*, 1999, **213**(D1), 59–71.
5 **Lee, M. M. K., Pine, T.** and **Jones, T. B.** Automotive box section design under torsion. Part 1: finite element modelling strategy. *Proc. Instn Mech. Engrs, Part D: J. Automotive Engineering*, 2000, **214**(D5), 347–359.
6 **Lee, M. M. K., Pine, T.** and **Jones, T. B.** Automotive box section design under torsion. Part 2: behaviour and implications on weight reduction. *Proc. Instn Mech. Engrs, Part D: J. Automotive Engineering*, 2000, **214**(D5), 473–485.
7 **Detwiler, D.** Computer aided structural optimization of automotive body structure. SAE paper 960523, 1996.
8 **Nishio, S.** and **Isgarashi, M.** Investigation of car body structural optimization method. *Veh. Des.*, 1990, **11**(1), 79–86.
9 **Kim, T.** Study on the stiffness improvement of bus structure. SAE paper 931995, 1993.
10 **Kim, M. H., Suh, M. W.** and **Bae, D. H.** Development of an optimum design technique for the bus window pillar. *Proc. Instn Mech. Engrs, Part D: J. Automotive Engineering*, 2001, **215**(D1), 11–20.
11 **Sun, L., Xie, J., Yu, C.,** *et al.* Study on dynamic modelling of automobile body structure. *Jixie Gongcheng Xuebao/Chin. J. Mech. Engng*, 1999, **35**(5), 72–74.
12 **Feng, G.** Finite element analysis for bus body structure. *Jixie Gongcheng Xuebao/Chin. J. Mech. Engng*, 1999, **35**(1), 91–95.